GROUND-STATE PROPERTIES OF BORON-DOPED DIAMOND

E. Yu. Zarechnaya [a,b*], *E. I. Isaev* [a,c**], *S. I. Simak* [c], *Yu. Kh. Vekilov* [a],

L. S. Dubrovinsky [b], *N. A. Dubrovinskaia* [d], *I. A. Abrikosov* [c]

[a] *Moscow State Institute of Steel and Alloys (Technological University)*
119049, Moscow, Russia

[b] *Bayerisches Geoinstitut, University of Bayreuth*
95440, Bayreuth, Germany

[c] *Department of Physics, Chemistry, and Biology (IFM), Linköping University*
SE-581 83, Linköping, Sweden

[d] *Mineralogisches Institut, University of Heidelberg*
D-69120, Heidelberg, Germany

Boron-doped diamond undergoes an insulator–metal or even a superconducting transition at some critical value of the dopant concentration. We study the equilibrium lattice parameter and bulk modulus of boron-doped diamond experimentally and in the framework of the density functional method for different levels of boron doping. We theoretically consider the possibility for the boron atoms to occupy both substitutional and interstitial positions and investigate their influence on the electronic structure of the material. The obtained data suggest that boron softens the lattice, but softening due to substitutions of carbon with boron is much weaker than due to incorporation of boron into interstitial positions. Theoretical results obtained for substitution of carbon are in a very good agreement with our experiment. We present a concentration dependence of the lattice parameter in boron-doped diamond, which can be used for an identification of the levels of boron doping in future experiments.

PACS: 61.05.cp, 61.72.S-, 71.20.-b, 74.70.Ad

1. INTRODUCTION

Diamond is a wide-band gap semiconductor, which is well known for its extreme hardness, chemical inertness, and high thermal conductivity. Increasing interest in studies of both doped natural diamonds and high-level doped synthetic diamonds [1] is caused by a discovery of profound influence of dopants on their physical properties. In particular, doping diamond with boron leads to the insulator–metal transition [2]. It was shown in Ref. [3] that the behavior of doped diamonds can be described in terms of one acceptor, and the boron appeared as a likely candidate for the acceptor center. Electric conductivity measurements of diamond revealed that for boron concentrations higher than some critical value n_c, estimated as 2.21 at. %, the

conductivity on the metallic side of the transition at low temperature followed a T^m law. For just-metallic samples, m was found to be $1/3$, tending to $1/2$ at higher concentrations [2]. There was some uncertainty in predictions of n_c above which metallic conduction occurred [2, 4–7].

A sharp superconducting transition near 4 K for diamond with high boron concentration ($n_B = 2.27$–2.84 at. %) in samples synthesized at high pressure (8–9 GPa) and high temperature (2500–2800 K) was recently reported in [8]. In previous studies of boron-doped thin films, a direct influence of the boron concentration on the hole–phonon coupling strength and the superconducting transition temperature T_c was obtained [4–6]. The phenomenon was studied theoretically from first principles within the so-called virtual crystal approximation [4, 9, 10].

[*] E-mail: ezarechnaya@yahoo.com
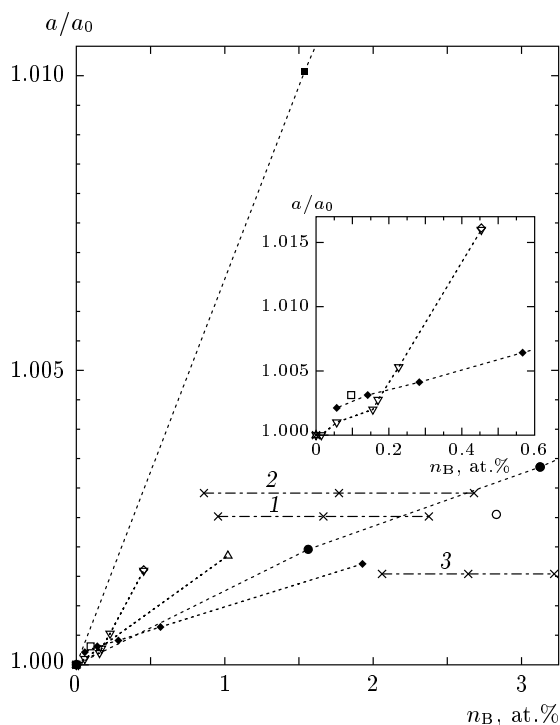[**] E-mail: eyvaz_isaev@yahoo.com

Fig. 1. Relative variation of the lattice parameter in boron-doped diamomd as a function of the boron concentration n_B (a_0 is the theoretical equilibrium lattice parameter of undoped diamond). Crosses denote our experimental results; solid circles and solid squares correspond to calculated supercells with boron at substitutional and interstitial positions, respectively. The experimental results reported earlier are also shown for comparison: $\circ$, $\triangle$ — [5]; $\square$ — [14]; $\diamond$ — [15]; $\triangledown$ — [16]; $\blacklozenge$ — [17]. The inset magnifies the low-concentration region for clarity

The electronic structure of boron-doped diamond (BDD) has also been studied using both experimental [6, 7] and *ab initio* supercell methods [8, 11]. X-ray absorption and emission spectroscopy measurements for metallic ($n_B = 0.1$ at. %) and semiconducting (0.03 at. % B and N) doped diamond films have shown a metallic partial density of states. From the X-ray absorption spectrum of BDD, the impurity states near the Fermi level have been attributed to boron. The experimentally observed strong hybridization between boron $2p$ states and carbon $2p$ states has been supported by calculations, which used the discrete variational X_α method [6]. In summary, it has been shown experimentally that for heavily boron-doped samples, the valence band near the Fermi level had a degenerate-metal picture in contrast to the impurity band model [12] and the holes-in-the-valence band model [13].

We emphasize that although the doping level is of crucial importance for the properties of BDD, its experimental determination is a nontrivial task. Most often, the boron composition is obtained from the concentration dependence of the lattice parameter. But as can be seen from Fig. 1, there is no agreement between the data available in the literature. Experimental data on the dependence of the lattice parameter on the boron concentration in diamonds synthesized by different methods (high pressure and high temperature doping or chemical vapor deposition) and studied by different groups (Refs. [5, 14–17]) differ substantially from each other. In Ref. [14], a decrease in the lattice parameter with an increase in the boron content up to 0.1 at. % was observed; above this value, the lattice parameter increased, which was interpreted as the effect of incorporation of boron into interstitial sites [14]. In other papers [15, 16], only the increase in the lattice parameter with the increase in the boron content was reported. The results obtained in Ref. [16] were compared with the predictions of Vegard's law, which assumes that changes in the lattice parameter are proportional to the impurity concentration. This law turned out to perfectly match the behavior of the lattice parameter of the BDD for boron concentrations below 0.15 at. % studied in Ref. [16]. Subsequently, secondary-ion mass spectroscopy was used in [17] for measurements of the boron content, which showed that the internal strain introduced by substitutional boron atoms is smaller than that expected from Vegard's law. At the same time, there are some uncertainties in the interpretation of the results of secondary-ion mass spectroscopy and X-ray microprobe measurements. Because both methods provide the data on the total amount of boron in a sample, it is difficult to distinguish between boron related to BDD and the possible boron-containing precipitates [18]. As a matter of fact, the purity of samples is often controlled by the X-ray diffraction measurements, which in many cases does not allow detecting a small amount of impurity phases. But their presence in the sample can seriously affect the interpretation of secondary-ion mass spectroscopy and X-ray microprobe results.

Possible aggregation of boron atoms in diamond was studied in Ref. [19]; the authors concluded that a pair of interstitial boron atoms was energetically unstable and should be excluded. Moreover, the pair was not a shallow acceptor in contrast to the results of ARPES [7] and X-ray experiments [6]. At the same time, experimental and theoretical studies confirmed that in the case of BDD with high level of doping, boron atoms could occupy interstitial positions in contrast to lightly

doped diamond, where boron is believed to substitute carbon atoms [6, 10, 20].

Based on the discussion above, and in the absence of consistency between available experimental data, we can expect that besides the boron content, there are additional factors (for example, poor stress relaxation in diamonds synthesized by both high-pressure–high-temperature doping and chemical vapor deposition) that influence the unit cell parameter of BDD. This strongly motivates theoretical calculations of the ground-state properties of BDD. Although it is unlikely that theory can account for all possible factors that influence the properties of BDD, it can supply experimentalists with helpful information on the ideal case, which can be used for the proper interpretation of many interesting phenomena (in particular, superconductivity) observed in BDD.

In this paper, we systematically investigate the BDD matrix. We present the results of our combined theoretical and experimental studies of equilibrium lattice parameters and bulk moduli of BDD at different boron concentrations. Theoretically, we consider boron at the substitutional as well as in the interstitial positions, and study its influence on the electronic structure of the material. From the comparison of the theoretically determined concentration dependence of the bulk modulus with our experimental data we conclude that the model where boron atoms occupy substitutional positions is in better agreement with experiment. Our concentration dependence of the lattice parameters calculated for this model can therefore be used for an identification of the boron doping level in future experiments.

2. EXPERIMENTAL METHOD AND DETAILS OF CALCULATIONS

A series of BDD samples was synthesized using a high-pressure and high-temperature technique described elsewhere [18, 21]. The samples were studied by the X-ray powder diffraction method using a high-brilliance FRD RIGAKU diffractometer (MoK_α radiation, 60 mA, 55 kV, APEX CCD area detector) [22]. High-purity gold (99.99995 % purity, Good Fellow Inc.) was used as the internal standard. Uncertainty in the determined lattice parameters was not worse than 0.0001 Å. The compressibility of one of these samples [23] was measured using the diamond anvil cell technique and synchrotron radiation. The chemical composition and texture of the samples were studied using a LEO-1530 scanning electron microscope. For

quantitative chemical analysis, a Camebax SX50 microprobe analyzer employing a PAP (Pouchou−Pichoir method) correction procedure was used.

In our studies, the doping of diamond by boron was simulated using a number of supercells with up to 64 atoms, where one carbon atom was substituted by a boron atom (B_C) or one boron atom was located in an interstitial position (B_I). Total energy calculations for the supercells were performed using the all-electron projector augmented waves method [24, 25] implemented in the Vienne *ab initio* simulation package [26]. Plane waves with the kinetic energy up to 400 eV were used in the expansion of the electron wave function in a periodic crystal. We also carried out convergence tests with respect to the cut-off energy. It was found that the total energy calculated for the cutoff value 900 eV differed by only 1.2 meV from the one calculated with the kinetic energy cutoff 400 eV. Thus, the latter value was found to be sufficient for theoretical determination of the lattice parameter. Exchange-correlation effects were treated by means of the generalized gradient approximation [27]. Integration over the Brillouin zone was performed by means of the linear tetrahedron method with Blöchl's correction [28]. The total energy calculations for supercells containing 8 and 16 atoms were carried out with $8 \times 8 \times 8$ k-point mesh; for 32- and 64-atom supercells, the number of k-points in the Brillouin zone was reduced to $6 \times 6 \times 6$. The convergence of the total energy with respect to k-points was better than 0.5 meV/atom. The Hellman−Feynman force theorem was used to minimize the total energy with respect to internal relaxations. Forces acting on each atom were converged with tolerance 10^{-3} eV/Å.

3. RESULTS AND DISCUSSION

Experimental and calculated lattice parameters and bulk moduli of pure diamond and BDD as a function of the boron content are shown in Figs. 1–3. From the microprobe analysis for BDD samples synthesized from B_4C/C mixture, we obtained the boron-concentration values 1.67(0.71) at. %, 1.77(0.91) at. %, and 2.64(0.58) at. % (averaged over at least 70 data points, with standard deviations given in parenthesis). The respective lattice parameters are 3.57598(12) Å, 3.5774(1) Å, and 3.5725(2) Å (Fig. 1). In principle, angle-dispersive microprobe analysis allows determining boron content quite precisely (within 0.2 at. %), even in the carbon matrix. But as was discussed in Refs. [18, 21], significant uncertainties in the determination of the boron concentration in BDD are related to

a contamination of the material by boron carbides B_4C and $B_{50}C_2$, which occurs in any currently known high-pressure and high-temperature synthesis experiments. According to X-ray powder diffraction, our samples contain about 2 wt. % of B_4C. The electron microprobe beam excites about 1 μm^3 of the sample material, and unevenly distributed submicron-size grains of carbide result in significant point-to-point variations of boron concentrations.

From our *ab initio* calculations, we obtained the lattice parameter $a = 3.573\,Å$ and the bulk modulus $B = 429$ GPa for pure diamond using the third-order Birch−Murnaghan equation of state [29], in good agreement with experimental values ($a = 3.567\,Å$ [30] and $B = 443$ GPa [31, 32]). We have found that the lattice parameter and the bulk modulus are affected differently by the boron doping depending on whether the boron position in the crystal is substitutional or interstitial. The lattice parameter of BDD with boron in an interstitial position tends to be larger compared to the substitutional case, irrespective of the supercell size at a given boron concentration n_B (see Fig. 1). For example, for $n_B = 3.1$ at. % in diamond, the expansion of the lattice is about $0.34\,\%$ for the substitutional position, which is in good agreement with the result in Ref. [19]. At the same time, the expansion is about $1.9\,\%$ for a similar concentration of boron placed in the interstitial positions. Unfortunately, it is difficult to directly compare theoretical data on the lattice parameter with the experimental data because of the total inconsistency of the latter.

We also compared our results with Vegard's model. Using experimental values of densities for diamond $(3.51\ g/cm^3)$ and B_4C $(2.48\ g/cm^3)$, the molar volumes of the compounds were obtained. These data were recalculated to the volumes of unit cells corresponding to the diamond structure (Fig. 2). A perfect agreement is observed between Vegard's law and the theoretically investigated dependence of the lattice parameter on the boron concentration for substitutional impurities at low doping levels (less than 2 at. %). At higher boron concentration, *ab initio* theory predicts small negative deviations of the concentration dependence of the lattice parameter from Vegard's law, as can be seen in Fig. 2.

For the substitutional positions of boron impurities, we also found a linear dependence of the bulk modulus on the boron concentration in diamond (Fig. 3). Recent experimental observations [23] suggested small changes in the bulk modulus in BDD in comparison with pure diamond. In fact, the experimentally obtained bulk modulus of pure diamond is 443 GPa [31, 32] versus 436 GPa for BDD investigated in Ref. [28], which cor-
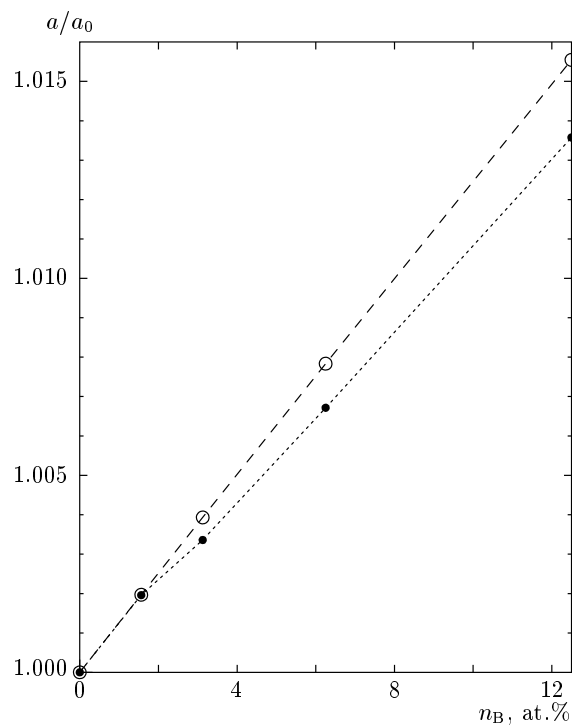

Fig. 2. Concentration dependence of the lattice parameters ratio for boron-doped diamond (a) and diamond (a_0), calculated from the first principles for substitutionally doped samples (solid filled circles) and obtained by Vegard's law (open circles)

responds to a weak decrease in the bulk modulus by about $1.58\,\%$.

We note that the sample examined in that work corresponds to the one denoted by number 3 in our experimental results presented in Fig. 1. In view of a large error in the determination of the boron content, the position of this experimental point in Fig. 3 can be located at the concentration as low as 2 at. %. This gives an estimation of the maximum effect of the boron doping on the bulk modulus of BDD, which is rather weak. According to the results of our calculations, the interpolated bulk modulus for substitutional boron doping at the doping level of 2 at. % is 421 GPa, and the decrease in the bulk modulus is only about $1.87\,\%$, in good agreement with the experiment. On the contrary, the interstitial boron doping leads to a much larger decrease in the bulk modulus down to 401.5 GPa at the same doping level or by $6.04\,\%$. Thus, the calculated values of the bulk modulus obtained in the model with substitutional boron are in a much better agreement with the experiment. A relatively sharp decrease in the bulk modulus with increasing boron concentration obtained within the model of interstitially doped
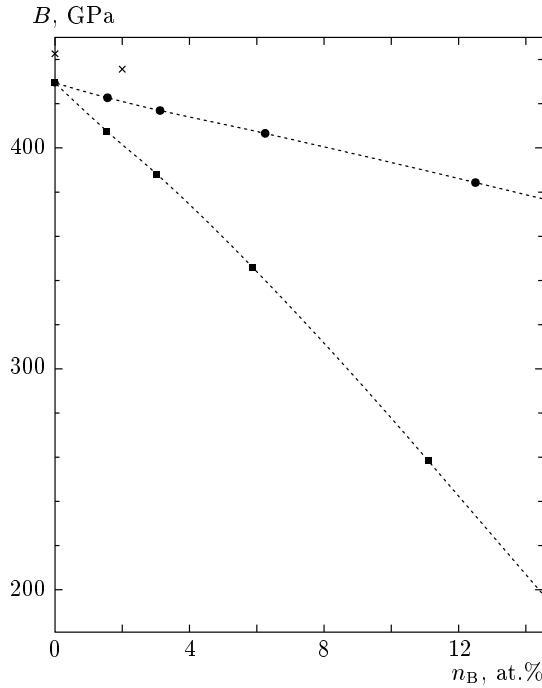
Fig. 3. Dependence of the bulk modulus on the boron concenration. Experimental results obtained in this paper are shown with crosses; the error bars for the determination of the boron concentration are the same as in Fig. 1. Calculated results of the bulk moduli for BBD with substitutional (circles) and interstitial (squares) boron impurities are also shown

Table 1. The equilibrium lattice parameter a_0 obtained from the total energy calculations for BBD in the substitutional and interstitial impurity positions. The unrelaxed case, a_0^{unrel}, corresponds to calculations with all the atoms at the sites of the ideal diamond lattice (including the interstitial positions). In the relaxed case, a_0^{rel}, internal positions in the supercell were optimized, and therefore the forces acting on all the atoms are nearly zero

System	n_B, at. %	a_0^{unrel}, Å	a_0^{rel}, Å
Substitutional B atom	1.563	3.580	3.580
	3.125	3.586	3.585
	6.25	3.598	3.597
	12.5	3.623	3.622
Interstitial B atom	1.538	3.609	3.609
	3.03	3.639	3.640
	5.88	3.700	3.703
	11.1	3.820	3.842

Table 2. Bond length $l_{B–C}$ between a boron atom and the nearest carbon atom, its change $\triangle$ in comparison with the ideal case in absolute values, and the relative change (in %) calculated for two models, with substitutional and interstitial boron atoms

System	n_B, at. %	$l_{B–C}$, Å	$\triangle$	$\triangle$, %
Substitutional B atom	1.563	1.590	0.043	2.78
	3.125	1.593	0.046	2.97
	6.25	1.598	0.051	3.30
	12.5	1.597	0.050	3.23
Interstitial B atom	1.538	1.576	0.029	1.87
	3.03	1.581	0.034	2.20
	5.88	1.591	0.044	2.84
	11.1	1.567	0.020	1.29

diamond might be considered as a consequence of the phonon softening in the C + B_I system. In fact, our preliminary calculations show that there are imaginary frequencies for some phonon modes of an 8-atom cubic diamond matrix with a cell-centered boron atom. We note that the cell was fully optimized with respect to the cell parameters and atomic coordinates.

In Tables 1–3, the effect of local atomic relaxations on the lattice parameters and total energies of the investigated systems is presented. We find that the ideal C–C bond length does not change considerably (Table 2). In fact, the change is about 3 % of the ideal bond length for substitutional boron, and about 2 % in the case of interstitial boron. The relatively small local displacements of atoms off the ideal lattice sites are in agreement with the results obtained for similar systems, e. g., (Ga, Mn)As [33, 34]. But because bonds are much stiffer in diamond, the contribution to the total energy due to local lattice relaxations is significant (Table 3). The total energy difference between relaxed and unrelaxed 64-atom supercells with one boron atom in the substitutional position is about −150 meV; for the interstitial boron atom, the difference is an order of magnitude larger, about −1729.5 meV. In particular, our preliminary estimates show that the impurity solution energy may decrease by about 25 % for the interstitial boron atom and by more than 50 % for the substitutional boron atom compared to calculations that do not take local lattice relaxations into account. We conclude that any simulations of the boron doping in diamond must include the effect of local relaxations.

Table 3. Contribution to the total energy of BBD due to local lattice relaxations (the relaxation energy E^{rel}) calculated for two models, with substitutional and interstitial boron atoms

System	n_B, at. %	E^{rel}, eV
Substitutional B atom	1.563	-0.1503
	3.125	-0.1500
	6.25	-0.1653
	12.5	-0.0949
Interstitial B atom	1.538	-1.7295
	3.03	-1.1723
	5.88	-0.5864
	11.1	-0.1190

We studied the electronic structure of BDD with the boron atoms in the substitutional and interstitial positions for fully relaxed supercells with 32 and 64 atoms. The calculated densities of electron states also behave differently for substitutional and interstitial boron atoms. The results of calculations are presented in Figs. 4 and 5, where we show the density of states for 64-atom supercells. This corresponds to the boron concentration 1.563 at. % for substitutional and 1.538 at. % for interstitial positions of the impurities. We have to note that the calculated band gap about 4.0 eV is 30 % smaller than the experimental one, as expected for standard density-functional-theory calculations. It slightly changes with doping.

In accordance with experiment [7] and previous theoretical observations [11], our calculated density of states for the substitutional boron atoms demonstrates a metallic character, with a finite number of electron states at the Fermi level. The valence band width 21 eV is slightly changed by doping with boron atoms, which introduces holes in the diamond valence band, and pushes bands up. We see that for BDD with $n_B = 1.563$ at. % with boron in the substitutional positions, a shallow acceptor band lies in a few tenths of electronvolt above the Fermi level and has the band width 0.5 eV, in good agreement with experiment (0.37 eV [35]) and previous theoretical data (0.60 eV for $n_B = 2.6$ at. % [11]). The value of the total density of states at the Fermi level in our calculations is 0.029 state per eV per diamond unit cell, which is very close to the values about 0.03 state per eV per diamond unit cell reported in Refs. [8, 11]. We find that local lattice relaxations due to the presence of a substitutional
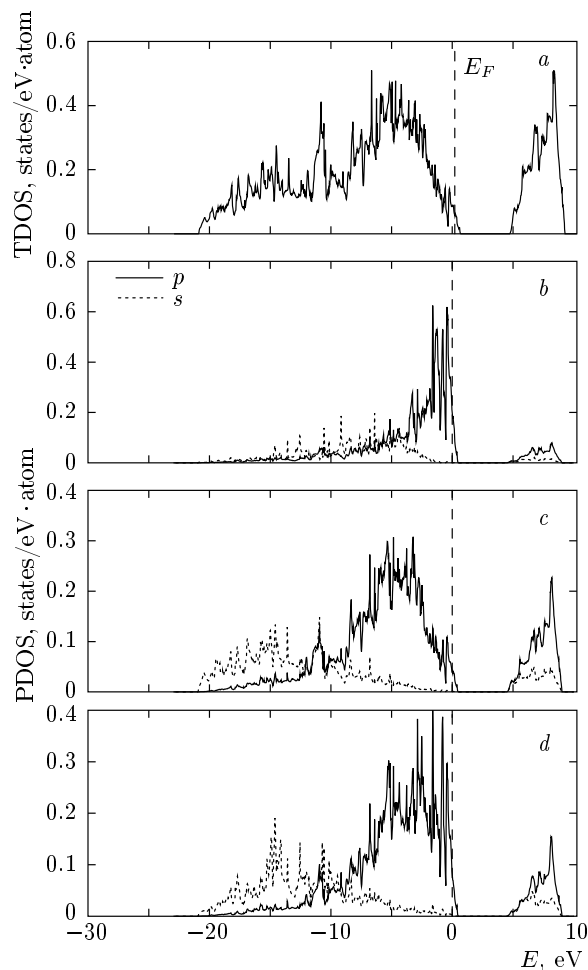

Fig. 4. Total (TDOS, a) and partial local density of states (PDOS) at a boron atom in the substitutional position (b), a carbon atom nearest to the boron atom (c), and a carbon atom most distant from the boron atom (d) calculated for 64 atoms supercell. All ionic positions are fully relaxed. Energy is given relative to the Fermi energy

boron atom lead to very small changes in the electronic structure of the material. The value of the total density of states at the Fermi level calculated for the supercell with all the atoms placed at the ideal positions of the diamond lattice is 0.063 eV, and the width of the acceptor band is larger by about 0.1 eV compared to the calculations with fully relaxed ionic positions.

We next compare our calculated atom-projected density of states for boron and carbon for the system with 1.563 % of boron atoms at substitutional positions in diamond. We find that the local density of states for the boron atom at the Fermi level is two times larger than for p-electrons at carbon atoms. From Fig. 4, we
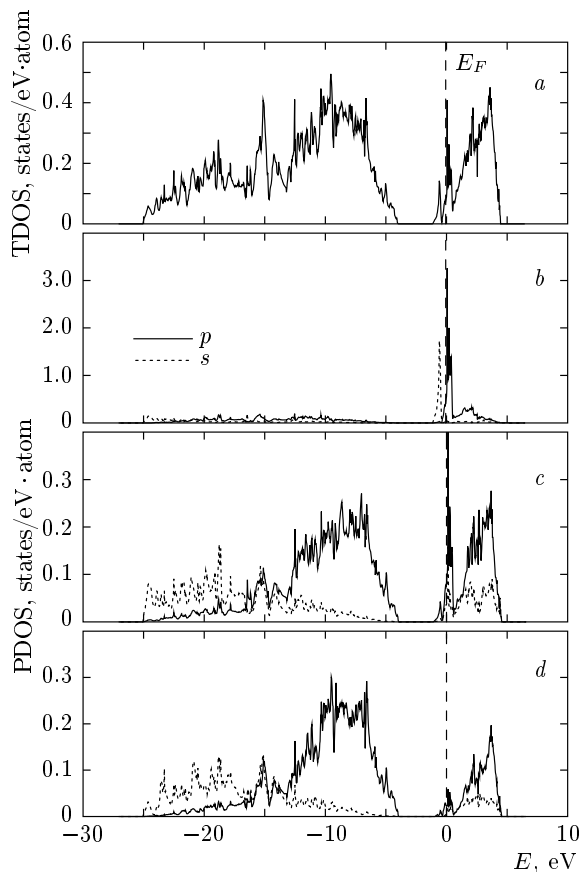
Fig. 5. The same as in Fig. 4 for a boron atom in the interstitial position

can clearly see the delocalized character of the holes introduced by the boron doping. Indeed, from comparison of Figs. 4c and 4d, where we show the density of states at the carbon atoms that are nearest to and more distant from the boron impurity, we conclude that the acceptor states are almost unchanged between these two atoms. The delocalized character of the hole states is in agreement with metallic behavior of BDD with high level of doping [7, 11].

It follows from Fig. 5 that in contrast to samples with substitutional impurities, an interstitial boron atom induces additional states in the band gap for the bulk diamond. This is due to completely saturated chemical bonds in diamond, which force electrons from the boron atom to form a donor state. Because of the high level of doping, the states form a narrow band.

From the atom-projected density of states, we conclude that neither the s- nor the p-electrons of boron contribute to the valence band density of states (states in the energy range from -4 to -25 eV in Fig. 5), in contrast to the case with the substitutional boron. It is

easy to see from Fig. 5b that the s- and p-electrons of boron are well separated near the Fermi level and the boron p-electrons form a donor band with the width about 0.5 eV for 1.538 at. % of the interstitial boron. Boron s-electrons form their own donor subband 1 eV below the Fermi level. The local density of states for carbon atoms shows that the s- and p-electrons in the valence band are also separated and their shape is very close to that of carbon in the substitutional case. Comparing the density of states at the carbon atoms that are nearest or distant neighbors of the boron interstitial impurity (Figs. 5c and 5d), we can see that boron-induced donor states are quite localized at boron sites. Indeed, there is a substantial contribution from these states at neighboring carbon atoms but it virtually disappears for distant atoms.

Therefore, the obtained results for systems with substitutional boron atoms are in better agreement with experiment. To the best of our knowledge, there are no experimental reports on the donor states in BDD, which makes the presence of individual interstitial boron atoms in the samples rather unlikely.

4. CONCLUSIONS

In summary, we have carried out combined experimental *ab initio* studies of the influence of boron doping on the equilibrium lattice parameter and the bulk modulus of diamond. The calculated dependences of the ground-state parameters on the dopant concentration can be used for an interpretation of experimental results. The calculations show an increase in the lattice parameter with increasing boron concentration with a larger slope in the case of interstitial impurities compared to samples with boron atoms at substitutional positions. The effect of ionic relaxations on the lattice parameter for all supercells under consideration is found to be small, although the local lattice relaxations contribute considerably to the total energy of BDD. It was found that substitutional and interstitial boron atoms affect ground-state properties and the electronic structure in different ways. The electronic structure changes significantly near the Fermi level. The electrons of a substitutional boron atom form acceptor bands, while the donor bands are observed for interstitial boron atoms. Based on the comparison of the results of calculations with experimental data, we conclude that the boron atoms substitute the carbon atoms in diamond rather than occupy interstitial positions. We note, however, that we considered only isolated boron

interstitial impurities in the diamond matrix. The presence of more complex defects cannot be excluded and their study should be of interest.

REFERENCES

1. Y. Haitao, Y. Haixue, and R. B. Jackman, Semicond. Sci. Technol. **20**, 296 (2005).

2. T. Tshepe, C. Kasl, J. F. Prins, and M. J. R. Hoch, Phys. Rev. B **70**, 245107 (2004).

3. A. T. Collins and A. W. S. Williams, J. Phys. C **4**, 1789 (1971).

4. L. Boeri, J. Kortus, and O. K. Anderson, Phys. Rev. Lett. **93**, 237002 (2004).

5. E. A. Ekimov, V. A. Sidorov, E. D. Bauer et al., Nature (London) **428**, 542 (2004); V. A. Sidorov, E. A. Ekimov, S. M. Stishov et al., Phys. Rev. B **71**, 060502(R) (2005).

6. J. Nakamura, E. Kabasawa, N. Yamada et al., Phys. Rev. B **70**, 245111 (2004).

7. T. Yokoya, T. Nakamura, T. Matsushita et al., Nature (London) **438** (2005).

8. H. J. Xiang, Z. Li, J. Yang et al., E-print archives, cond-mat/0406446.

9. K.-W. Lee and W. E. Pickett, Phys. Rev. Lett. **93**, 237003 (2004).

10. X. Blase, Ch. Adessi, and D. Connétable, Phys. Rev. Lett. **93**, 237004 (2004).

11. K.-W. Lee and W. E. Pickett, Phys. Rev. B **73**, 075105 (2006).

12. G. Baskaran, E-print archives, cond-mat/0404286.

13. J. Nakamura, T. Oguchi, N. Yamada et al., E-print archives, cond-mat/0410144.

14. B. V. Spitsyn, L. L. Bouilov, and B. V. Derjaguin, J. Cryst. Growth **52**, 219 (1981).

15. O. A. Voronov and A. V. Rakhmanina, Inorg. Mater. **29**, 707 (1993).

16. F. Brunet, P. Gremi, M. Pernet et al., Diamond Rel. Mater. **7**, 869 (1998).

17. E. Bustarret, E. Gheeraert, and K. Watanabe, Phys. Stat. Sol. (a) **199**, 9 (2003).

18. N. Dubrovinskaia, L. Dubrovinsky, N. Miyajima et al., Z. Naturforsch. B **61**, 1561 (2006).

19. J. P. Goss and P. R. Briddon, Phys. Rev. B **73**, 085204 (2006).

20. Yu. G. Pogorelov and V. M. Loktev, E-print archives, cond-mat/0405040.

21. N. Dubrovinskaia, G. Eska, G. A. Sheshin, and H. Braun, J. Appl. Phys. **99**, 033903 (2006).

22. L. Dubrovinsky, N. Dubrovinskaia, I. Kantor et al., High Press. Res. **26**, 2, 137 (2006).

23. N. Dubrovinskaia, L. Dubrovinsky, W. A. Crichton et al., High Press. Res. **26**, 79 (2006).

24. P. E. Blöchl, Phys. Rev. B **50**, 17953 (1994); G. Kresse and J. Joubert, Phys. Rev. B **59**, 1758 (1999).

25. P. E. Blöchl, Phys. Rev. B **50**, 17953 (1994).

26. G. Kresse and J. Furthmüller, Comp. Mater. Sci. **6**, 15 (1996); G. Kresse and J. Furthmüller, Phys. Rev. B **54**, 11169 (1996).

27. J. P. Perdew, J. A. Chevary, S. H. Vosko et al., Phys. Rev. B **46**, 6671 (1992).

28. P. E. Blöchl, O. Jepsen, and O. K. Andersen, Phys. Rev. B **49**, 16223 (1994).

29. O. L. Anderson, *Equation of State of Solids for Geophysics and Ceramic Science*, Oxford University Press, New York (1995).

30. K. Geshneider, Jr., in *Solid State Physics*, Vol. 16, ed. by F. Seitz, D. Turnbull, and H. Ehrenreich, Academ. Press, New York (1964), p. 275.

31. F. Occelli, P. Loubeyre, and R. Letoullec, Nat. Mater. **2**, 151 (2003).

32. N. Dubrovinskaia, L. Dubrovinsky, W. Crichton et al., Appl. Phys. Lett. **87**, 083106 (2005).

33. R. Shioda and K. Ando, Phys. Rev. B **58**, 1100 (1998).

34. M. Jain, L. Kronik, and J. R. Chelikowsky, Phys. Rev. B **64**, 245205 (2001).

35. F. Fontaine, J. Appl. Phys. **85**, 1409 (1999).